Transilvania University of Brasov
FACULTY OF MECHANICAL ENGINEERING

COMEC 2021

Brașov, ROMANIA, 21-23 October 2021

USING A FLOWER POLLINATION ALGORITHM TO OPTIMISE THE CROSS MEMBERS OF A TRUCK FLOOR

Szilárd Nagy[1], Károly Jármai[2]

[1] PhD student/designer engineer, University of Miskolc, Institute of Energy and Chemical Machinery, /Aventics Hungary Ltd, szilard.nagy@emerson.com

[2] Professor, University of Miskolc, Institute of Energy and Chemical Machinery, jarmai@uni-miskolc.hu

Abstract: *Longitudinal beams and cross members combine to form grillage or lattice constructions.. Grillages can be used to simulate car frames, bus floor frames, or the complete vehicle. This page explains how the structure's cross components were optimised. The flower pollination algorithm is a metaheuristic evolution technique for optimisation inspired by nature. Flower pollination performed well in comparison to many other metaheuristic evolutionary methods, which is why it was selected. The aim functions are the optimised cross-total member's weight and cost. The cross-sectional dimensions of the member remain unknown. The RHS portion has been optimised before, and this case was created for the I-section. Design constraints include local buckling of the webplate and flanges, as well as fatigue. In the calculations, aluminium alloys were employed. When the optimal solutions were examined, it was revealed that using I-sections saved both time and money.*
Keywords: *truck floor members, evolutionary optimisation, flower pollination algorithm, local buckling, fatigue*

1. INTRODUCTION

Vehicle structural design is critical in two ways: it decreases the size and cost of structural components while also enhancing other features like reliability and energy absorption. To demonstrate bulk reduction accomplishments, several types of studies [1, 2] have been published. Other materials have been used as a solution in some instances [3, 4, 5]. Although using lightweight aluminium or magnesium might save a lot of weight, it can be expensive. To determine the mass and cost optima, designers can employ a number of optimisation approaches [6, 7, 8, 9].
Cost concerns are becoming increasingly crucial in order to obtain a respectable outcome [10]. The other important sector for improving crashworthiness is increased collision energy impact [11, 12]. Some computer algorithms can simulate and improve collisions [13]. The energy impact of using alternative cross-sections, such as circular tubes, can be significant [14]. Using a more robust optimisation technique, crashworthiness modelling and design can be enhanced [15]. We also produced several steel structure simulations and designs as part of our research, intending to determine the best solution utilising a range of optimisation approaches [16].
A vehicle with various cross-sections constructed of aluminium was also explored [17]. The conclusion can be improved by employing a more thorough optimisation approach. Optimisation options include robot workspace design [18], which may be linked to vehicle component production, and manufacturing optimisation [19], which includes finding the best turning settings. Support grilles, also known as support grid-like structures, are commonly utilised in the automotive industry. This construction might be utilised to mimic car chassis, bus chassis, or even ship cellular plate architecture. If one considers fire safety, the application of intumescent paintings are also important [20].
In this article, we optimised an existing three-layer truck platform using a robust and recently built evolutionary method. We attempted to determine the optimum cross member sizes. The rest of the platform's components were unaffected. This also implies that the new geometric cross member will be able to take the place of the old one.

2. THE FLOWER POLLINATION ALGORITHM

The heuristic branch of artificial intelligence, which includes evolutionary algorithms, has gotten a lot of attention in recent years. This is to be expected, given its ability to solve non-linear, multi-variable advanced search and optimisation issues.
They can also be beneficial when using standard gradient techniques is problematic or impossible. The target function may also be thought of as a black box, which is a significant benefit. You do not need to understand the function's internal structure; all you need to know are the inputs and outputs. Apart from the benefits, one downside of their operation is that it is impossible to determine if the result obtained is a local or global minimum. It will be

introduced and utilised the Flower Pollination (FPA) method, which is one of the numerous evolutionary algorithms.
The pollination process in plants inspired the flower pollination algorithm (or FPA for short). This evolutionary method was proposed by Xin-She Yang [20], and it is still relatively young. The reproductive process of plants in nature is characterised by several pollination techniques. Insects, birds, bats, other creatures, and the wind all carry pollen from one plant to another. Some plants have developed their own pollination strategy.
In order to represent the process and give the mathematical foundation for the algorithm, four guiding principles can be specified in general:

- During global pollination, pollen is transferred from one individual to another (cross-pollination). To simulate pollinator movement, a random integer that matches the Lévy distribution might be utilised.
- In local pollination, pollen from the same flower or another bloom of the same plant is utilised. Pollen from the same species can only pollinate plants of the same species. According to the FPA, pollination will only take place if it produces a better outcome than what is already available.
- To represent the chance of local and global pollination, a standard distributed random real number is employed.

In mathematical form, cross-pollination is:

$$\bar{x}_i^{(G+1)} = \bar{x}_i^{(G)} + L\left(\bar{g}^* - \bar{x}_i^{(G)}\right) \tag{1}$$

where $\bar{g}^*$ is the global minimum found up to G and L is the Levy number approximated by the following formula [21, 22]:

$$L \approx \frac{\lambda \Gamma(\lambda) \sin\left(\frac{\pi\lambda}{2}\right)}{\pi} \frac{1}{s^{1+\lambda}} \tag{2}$$

where λ is a constant (recommended value: $\lambda = 1.5$), $\Gamma(\lambda)$ is a gamma distribution function, and $s > 0$ is a random step.
A well-known mutation formula from differential evolution can be used to express local pollination [23]:

$$\bar{x}_i^{(G+1)} = \bar{x}_i^{(G)} + \epsilon\left(\bar{x}_{r_1}^{(G)} - \bar{x}_{r_2}^{(G)}\right) \quad r_1 \neq r_2 \neq i \tag{3}$$

where $\epsilon \in [0; 1] \cup R$ is a random number of the normal distribution, r_1 and r_2 are random integers.

FPA, like other evolutionary algorithms, is designed to tackle continuous problems. The difficulties that emerge in engineering practice, on the other hand, are limited.

$$\begin{aligned} & \min \mathcal{F}(\bar{x}) \quad \bar{x} = [x_1, x_2 \cdots x_i \cdots x_D] \\ if \quad & g_j(\bar{x}) \leq 0 \quad 1 \leq j \leq q \\ & h_k(\bar{x}) = 0 \quad q+1 \leq k \leq r \\ & x_A \leq x_i \leq x_F \end{aligned} \tag{4}$$

where D is the number of variables in the problem, x_A and x_F are upper and lower limits.

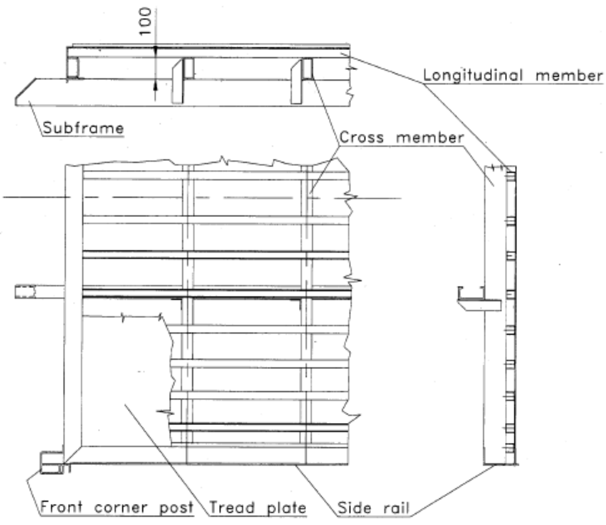

Figure 1. Structure of truck floor

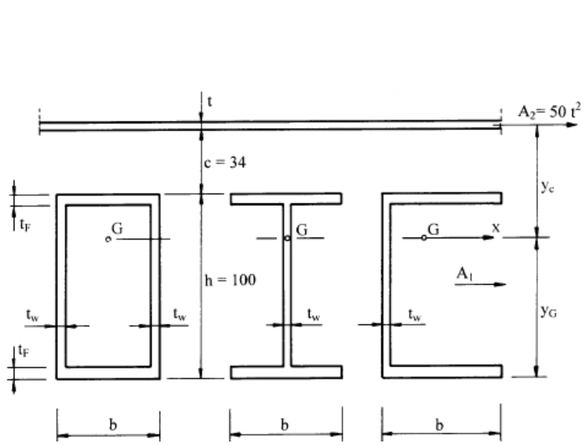

Figure 2. Cross-sectional dimensions of cross-members

It is necessary to make the non-continuous, limited problem continuous. The most common method in practice is to include a penalty parameter in the fitness function $F(x)$ that is minimised if the inequality or equality criterion is broken. If the requirements are satisfied, it is ideal to include the penalty function in such a manner that the fitness value does not change or is minimal. If not, raise the value by a factor of ten (this value is 106 in this article).

$$\alpha(x) = \begin{cases} 0 & if x \leq 0 \\ 10^6 & else \end{cases} \quad (5)$$

If the programming simulation environment allows it, it is common to add infinite, albeit it is not ideal. It is conceivable that the initial population will not include all of the individuals who fulfil the restrictions, in which case the optimisation will fail. We do not specify a penalty function for equality criteria because it is no longer required by the problem to be solved.

Using a penalty function to solve a continuous optimisation problem:

$$min\, \mathcal{F}(\bar{x}) + \sum_{j=1}^{q} \alpha\left(g_j(\bar{x})\right) \quad (6)$$

3. TRUCK FLATBED

The chassis of the vehicle in question is made up of two longitudinal steel beams in this example. A three-layer platform is linked to this through intermediary support (Figure 1). The three layers of the structure are cross members, longitudinal members, and floor slabs. AlMg2.5 [25] is used for the floorboard, while AlMgSi0.7 [24] is used for the cross-braces. A side frame surrounds the structure and carries the loads of neighbouring superstructures (roof, sidewalls, doors).

By altering the cross-sectional dimensions of the cross members, the goal of the optimization is to minimize the cost of the truck platform material. The cross-sectional dimensions are depicted and illustrated in Figure 2. For the tested original RHS (Rectangular Hollow Section) cross-sections, previous computations in [17] indicated that the I-section outperformed the I-section and C-section in terms of mass. As a result, the following computations were done only using this.

The effective width of the deckplate is $50t$, where t is the thickness of the deckplate. The following are the properties of the I-geometric section, including cross-sectional area, the center of gravity distances, and second-order torque:

$$A = A_1 + A_2; \quad A_1 = ht_w + 2bt_f; \quad A_2 = 50t^2 \quad (7)$$

$$y_G = \frac{A_1}{A}\left(\frac{h+t}{2} + c\right); \quad y_c = h + c + \frac{t}{2} - y_G \quad (8)$$

$$I_x = \frac{h^3 t_w}{12} + \frac{bt_f h^2}{2} + A_1\left(y_c - \frac{h}{2}\right)^2 + A_2 y_G^2 \quad (9)$$

The fitness function of optimisation, according to the symbols (7) to (9) and the previously mentioned aims, is:

$$\mathcal{F}(\bar{x}) = \rho A_1 L_c n_c; \quad \bar{x} = [b, t_f] \quad (10)$$

where $\rho = 2{,}7x10^{-6}\, kg/mm^3$ is the density of aluminium, L_c = 2440 mm is the length of a cross member, and n_c is the number of cross members.

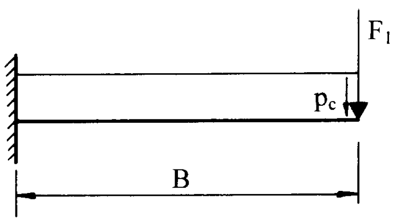

Figure 3. Mechanical model of cross-member semi-console

Only the typical size of the belt plate vary as can be observed. The height of the backboard h = 100 mm is the same as the original RHS profile. Thickness t_w = 3.4 mm is the minimum required for manufacturing. Due to the superposition of two power systems, the load on the crossbars may be described as a bending moment and a shear force (Figure 3). The initial force mechanism dispersed the burden due to the payload's weight.

$$p = \frac{F_p n_p}{BL} \quad (11)$$

where F_p = 8500 N represents the assumed weight of the pallets, n_p = 5 represents the number of pallets placed, B = 720 mm represents the typical dimensions of the semi-cantilevered platform, and L represents the typical dimensions of the semi-cantilevered platform. Per cross member, the load is distributed along a line:

$$p_c = \frac{pL}{n_c - 1} \quad (12)$$

The concentrated force is the second force system, which is due to the weight of the superstructure. F1 = 1946N. The bending moment is most significant in the horizontal position.

$$M_h = \frac{p_c B^2}{2} + F_1 B = \frac{F_p n_p B}{2(n_c - 1)} + F_1 B \quad (13)$$

the shear force

$$Q = \frac{F_p n_p}{n_c - 1} + F_1 \quad (14)$$

and bending stress

$$\sigma = \frac{M_h}{I_x} \max(y_G, y_C) \quad (15)$$

$$\tau = \frac{Q}{h t_w} \quad (16)$$

The failure statuses can be used to determine the optimisation's limits. The fatigue limit of the welds is the first such limitation. The Eurocode 3 [26] and the Recommendations [27] have notable discrepancies. The main one [27] is capable of handling both steel and aluminium. At [26], the cut-off limit is 10^8 cycles, but at [27], it can go up to 10^9 cycles. The fatigue design of aluminium buildings is governed by Eurocode 9 [28]. Steel and aluminium fatigue limits are listed in the same FAT classes in [27]. It simplifies the calculations and possible comparisons. The permissible stresses are σ_C=28 MPa and τ_c=28 MPa shear stress at $2x10^6$ cycles, according to [27]. This value represents the actual number of cycles $N = 2x10^5$.

$$log\Delta\sigma_N = \frac{1}{3} log\frac{2x10^6}{N} + log\sigma_C \quad (17)$$

$$log\Delta\tau_N = \frac{1}{3} log\frac{2x10^6}{N} + log\tau_C \quad (18)$$

and the limits are expressed in equations (19) to (25)

$$g_1(\bar{x}) = \frac{\gamma_{Mf}\sigma}{\Delta\sigma_N} - 1 \leq 0 \quad (19)$$

$$g_2(\bar{x}) = \frac{\gamma_{Mf}\tau}{\Delta\tau_N} - 1 \leq 0 \quad (20)$$

where $\gamma_{Mf} = 1.25$.

The stability conditions impose further restrictions. Because of the deckplate's state,

$$g_3(\bar{x}) = \frac{\beta h}{22 t_w \varepsilon} - 1 \leq 0 \quad (21)$$

where β and ε can be calculated as follows

$$\beta = \begin{cases} 0{,}65 + 0{,}35\frac{y_0}{y_c} & if 1 > \frac{y_0}{y_C} \geq 0 \\ 0{,}65 + 0{,}30\frac{y_0}{y_c} & if 0 > \frac{y_0}{y_C} \geq -1 \end{cases} \quad (22)$$

$$\varepsilon = \sqrt{\frac{250}{\sigma/\gamma_{M1}}} \quad (23)$$

$$y_0 = y_G - \frac{t}{2} - c \quad (24)$$

local buckling constraint for the flange plate

$$g_4(\bar{x}) = \frac{b}{14 t_f \varepsilon} - 1 \leq 0 \quad (25)$$

4. THE RESULTS OF THE OPTIMISATION

In the optimization, n_c = 8,10,12,14,16 cross members were employed. The findings are summarised in Table 1. The I-section with optimised proportions saves weight and money as compared to the original RHS part.
All of the required cross-braces are included in the material cost.

$$K_m = k_m m_c = k_m \rho A_1 n_c L_c \tag{26}$$

k_m = 1.72 $/kg [29] is the cost of the specific substance. The cost of tooling has been omitted since it has little impact on the cost of material per support, according to previous research by [17].

Table 1. Optimisation results

	Original RHS section [17]				I-section optima			
n_c	14	12	10	16	14	12	10	8
b [mm]	55,0	115,0	120,0	73,9	66,1	80,8	78,1	74,3
t_f [mm]	5,4	3,0	3,4	4,6	5,9	5,6	7,0	9,4
A_1 [mm^2]	1274	1370	1496	1019,88	1116,36	1246,57	1437,52	1738,32
Mass [kg]	117,50	108,31	98,56	107,50	102,96	98,55	94,70	91,62
Material cost [$]	202,10	186,28	169,51	184,90	177,09	169,50	162,89	157,58

As the number of cross members grows, the cross-sectional area decreases while the overall weight increases. The mass savings varied from 4 to 14 percent, depending on the number of cross members. By lowering the number of brackets, more significant savings may be realised when compared to the initial n_c = 10,12,14. Cost reductions varied from 4 to 15%, depending on the number of cross members. During optimisation, the fatigue condition of the welded joints was an active constraint. Fatigue becomes even more of a barrier as the number of load-cycles increases.

5. CONCLUSIONS

The cross-sectional area reduces as the number of cross members rises, but the overall weight increases. Depending on the number of cross members, mass savings varied from 4 to 14 percent. The number of brackets can be decreased to save money when compared to the original n_c = 10,12,14. Depending on the number of cross members, cost reductions ranged from 4 to 15%. The fatigue condition of the welded joints was an active constraint during optimisation. As the number of load-cycles rises, fatigue becomes a more significant restriction.
In the optimisation presented, the cross-sectional dimensions of drawn aluminium welded truck platforms were determined. The section plates' fatigue conditions and local buckling were both restricted. The flower pollination algorithm employed is quite dependable, and it did an excellent job at identifying the best option. The goal functions were the optimised cross-overall member's weight and cost. The use of I-shaped cross members has been considered. Compared to the original RHS sectional construction, it resulted in weight and cost reductions for each cross-component. The cost reductions varied from 4 to 15% depending on the number of cross members.

ACKNOWLEDGEMENT

The research was supported by the Hungarian National Research, Development and Innovation Office under the project number K 134358.

REFERENCES

1. Lukaczyk, T. et al. 2015, SUAVE: An Open-Source Environment for Multi-Fidelity Conceptual Vehicle Design, 16th AIAA/ISSMO Multidisciplinary Analysis and Optimization Conference, 22-26 June 2015, Dallas, TX, AIAA 2015-3087, 56 p.
2. Davis, E.A., Davis, B.P., Davis, R.A., 2011, Frame design for reduced-size vehicle, United States Patent, Patent No.: US 7.942,447 B2, Date of Patent: May 17, 2011, 51 p.
3. Hirsch, J., 2014, Recent development in aluminium for automotive applications, Transactions of Nonferrous Metals Society of China, 24(7), pp 1995-2002, https://doi.org/10.1016/S1003-6326(14)63305-7

4. Kiani, M., Gandikota, I., Rais-Rohanib, M., Motoyama, K., 2014, Design of lightweight magnesium car body structure under crash and vibration constraints, Journal of Magnesium and Alloys, 2(2), pp. 99-108.
5. Deb, A., Mahendrakumar, M.S., Chavan, C., Karve, J., Blankenburg, D., Storen, S., 2004, Design of an aluminium-based vehicle platform for front impact safety, International Journal of Impact Engineering, 30(8–9), pp. 1055-1079.
6. Yildiz, AR, 2008, Optimal Structural Design of Vehicle Components Using Topology Design and Optimisation. Materials Testing, 50(4), pp. 224-228. https://doi.org/10.3139/120.100880
7. Fenyes, P., 2012, Multidisciplinary design and optimisation of automotive structures-a parametric approach, 8th Symposium on Multidisciplinary Analysis and Optimization 06-08 September 2000, Long Beach, CA, USA. Published Online: August 22 2012, 12 p. https://doi.org/10.2514/6.2000-4706
8. Yildiz, BS, 2020, Optimal design of automobile structures using moth-flame optimisation algorithm and response surface methodology, Materials Testing, 62(4), pp. 371-377. https://doi.org/10.3139/120.111494
9. Demirci, E., Yildiz, AR, 2019, A new hybrid approach for reliability-based design optimisation of structural components. Materials Testing, 61(2), pp.111-119. https://doi.org/10.3139/120.111291
10. Lee, H., Olds, J.R., 1997, Integration of Cost and Business Simulation into Conceptual Launch Vehicle Design, Defense and Space Programs Conference and Exhibit Huntsville, AL, September 1997. AIAA 97-3911, 12 p.
11. Mayville, R.A., Johnson, K.N., Tyrell, D.C., String, R.G., 2008, Rail Vehicle Cab Car Collision and Corner Post Designs According to APTA S-034 Requirements, Paper No: IMECE2003-55114, pp. 45-51; ASME International Mechanical Engineering Congress and Exposition, November 15–21, 2003, Washington, DC, USA, May 12, 2008, https://doi.org/10.1115/IMECE2003-55114
12. Gu, L., Yang, R.J., Tho, C.H., Makowskit, M., Faruquet, O., Li, Y., 2004, optimisation and robustness for crashworthiness of side impact, 26(4), pp. 348–360, https://doi.org/10.1504/IJVD.2001.005210
13. Blumhardt, R., 2004, FEM - crash simulation and optimisation, International Journal of Vehicle Design, 26(4), pp. 331–347, https://doi.org/10.1504/IJVD.2001.005209
14. Zarei H.R., Kröger M., 2006, Multiobjective crashworthiness optimisation of circular aluminum tubes, Thin-Walled Structures, 44(3), pp. 301-308, https://doi.org/10.1016/j.tws.2006.03.010
15. Yildiz, A.R., Solanki, K.N., 2012, Multi-objective optimisation of vehicle crashworthiness using a new particle swarm based approach, International Journal of Advanced Manufacturing Technology 59, pp. 367–376, DOI 10.1007/s00170-011-3496-y
16. Farkas, J., Jármai, K., 2013, Optimum design of steel structures, Springer Verlag, Heidelberg, 265 p.
17. Farkas, J., Jármai, K., Dúl, R., 2001, Minimum cost design of a truck floor welded from aluminium-alloy profiles, Welding in the World, Pergamon Press, 45(9-10), pp. 19-22.
18. Aboulissane, B., El Bakkali L., El Bahaoui J., 2020, Workspace analysis and optimisation of the parallel robots based on computer-aided design approach, Facta Universitatis Series: Mechanical Engineering, 18(1), pp. 79 – 89, https://doi.org/10.22190/FUME190428006A
19. Jozić, S., Dumanić, I., Bajić, D., 2020, Experimental analysis and optimisation of the controllable parameters in turning of an AW-2011 alloy; dry machining and alternative cooling techniques, Facta Universitatis Series: Mechanical Engineering, 18(1), pp. 13 – 29. https://doi.org/10.22190/FUME191024009J
20. Száva Ioan, Jármai Károly, Vlase Sorin, Bondár Tibor, Ungureanu Valentin-Vasile, Gálfi Botond-Pál, Dani Péter and Munteanu Renáta: The Intumescent Paint Layer's Thickness Influence on the Load-Bearing Capacity of the Steel Joints, 2nd International Scientific Conference Structural and Physical Aspects of Civil Engineering, Technical University of Košice, Faculty of Civil Engineering, Slovak Society for Mechanics, SAS, November 27 - 29, 2013, High Tatras, Štrbské Pleso, Slovakia
21. Xin-She, Y., 2012, Flower pollination algorithm for global optimisation, Unconventional Computation and Natural Computation, 7445, pp. 204-249.
22. Xin-She, Y., 2010, Nature-Inspired Metaheuristic Algorithms Second Edition, Luniver Press, Frome,
23. Storn, R., Price, K., 1997, Differential Evolution – A Simple and Efficient Heuristic for global Optimisation over Continous Spaces, Journal of Global Optimization, 11, pp 341-359, doi.org/10.1023/A:1008202821328
24. DIN 1725-1983: Aluminiumlegierungen. Knetlegierungen, Knetlegierungen, 1983.
25. DIN 1748-1983: Strangpressprofile aus Aluminium und Aluminium-Knetlegierungen. Eigenschaften, Zulässige Abweichungen, 1983.
26. Eurocode 3, 2005, Design of steel structures Part 1.9. Fatigue, European Committee for Standardization, Brussels.
27. Hobbacher, A. 2007, IIW Recommendations for fatigue design of welded joints and components, IIW-doc, IIW-1823-07, ex XIII-2151r3-07/XV-1254r3-07
28. *Eurocode 9, 2007, Design of aluminium structures* - Part 1-3: *Structures* susceptible to fatigue. European Committee for Standardization, Brussels.
29. London Metal Exchange, www.lme.com/metals, access date: 2020.03.05